Structure of water layers on hydrogen-covered Pt electrodes

Tanglaw Roman and Axel Groß*
Institute of Theoretical Chemistry, Ulm University, D-89069 Ulm, Germany

The structure of water layers above hydrogen-covered Pt(111) surfaces at room temperature has been studied by ab initio molecular dynamics simulations based on periodic density functional theory calculations. Fully hydrogen-covered Pt(111) with additionally either a hydrogen vacancy or another hydrogen adatom have been considered. The resulting structures have been analyzed in detail as a function of the hydrogen coverage. In particular, the thermal disorder in the water layer is examined in terms of deviations from the ice lattice, orientational inhomogeneity within a water bilayer, as well as the onset of proton transfer. On hydrogen-covered Pt(111), the water layer is located at a much larger distance from the Pt atoms than on the pure metal surfaces. Surprisingly, the more weakly bound water layer on the hydrogen-covered Pt(111) electrode exhibits a greater order than the water layer on clean Pt(111) which is attributed to the stronger water-water interaction above hydrogen-covered Pt(111). The relevance of our findings for the understanding of electrochemical electrode/water interfaces is discussed.

Keywords: Computer simulations, density functional theory calculations, molecular dynamics, hydrogen, water, platinum, low index single crystal surface

I. INTRODUCTION

There is a renewed interest in the whole field of electrochemistry because of its relevance for future technologies in energy conversion and storage. At the same time, modern electrochemistry becomes increasingly concerned with the development of an atomistic understanding of electrochemical processes [1]. In spite of the complexity of electrochemical interfaces, theoretical studies can contribute significantly to the progress in this field [2] in a similar way this has already happened in the related field of surface science [3]. In particular electronic structure calculations based on density functional theory (DFT) calculations can nowadays elucidate the structures of complex interfaces [4]. And in fact, there have already been numerous studies addressing structures and processes at electrochemical solid-liquid interfaces within periodic DFT calculations taking also varying electrode potentials into account [5–17]. It is certainly true that these studies provided valuable insights into fundamental electrochemical processes at the atomistic level.

Still, it is also fair to say that in most of these theoretical studies little attention has been paid to the fact that as a function of the electrochemical conditions (electrode potential, pH, electrolyte) in equilibrium electrochemical interfaces are typically covered by specifically or non-specifically adsorbed species [1]. It is very likely that the presence of these adsorbed species has a severe influence on the structure of the electrochemical electrode-electrolyte interfaces and on the processes such as electrocatalytic reactions occurring at these interfaces.

It is well-known that under electrochemical conditions and low potentials Pt(111) is covered by hydrogen [18, 19]. There is still some controversy between experiment and theory regarding the hydrogen equilibrium coverage. Whereas experiments indicate that at 0 V relative to the normal hydrogen electrode (NHE) the hydrogen coverage should be about 0.66 ML [19], DFT calculations rather yield a hydrogen coverage of 1 ML [10, 20]. Still, there is a qualitative agreement that there is a significant hydrogen coverage. In the electrochemical literature, this strongly adsorbed hydrogen is typically referred to as underpotential deposited (upd) hydrogen [21].

Additionally, there is another weakly adsorbed hydrogen species which is also called overpotential deposited (opd) hydrogen [21]. The role of this opd hydrogen in the hydrogen electrocatalysis has just been intensively discussed from a theoretical point of view [22]. In particular on transition metal surfaces, this weakly bound species might play an important role in the hydrogen evolution reaction which is for example a crucial step in the electrolysis of water [23]. Clarifying the microscopic structure and the dynamics of the hydrogen layer on Pt(111) under realistic electrochemical conditions is therefore a prerequisite for an understanding of the mechanism underlying this important reaction.

It is true that there exist many molecular dynamics simulations addressing the structure of water/metal interfaces using classical force fields which usually reproduce bulk water structures rather well [24–27], however, which typically do not describe the water-metal interaction reliably. Ab initio molecular dynamics (AIMD) simulations have recently shown [17] that at room temperature water layers at close-packed hexagonal electrode surface such as Ag(111), Au(111), Pt(111) or Ru(0001) are not crystalline in an ice-like structure as was previously assumed [6, 28–31] but are rather disordered. This

*Corresponding author:
Institute of Theoretical Chemistry
Ulm University
D-89069 Ulm/Germany
Tel.: +49 (0)731 50 22810
Fax: +49 (0)731 50 22819
Email: axel.gross@uni-ulm.de

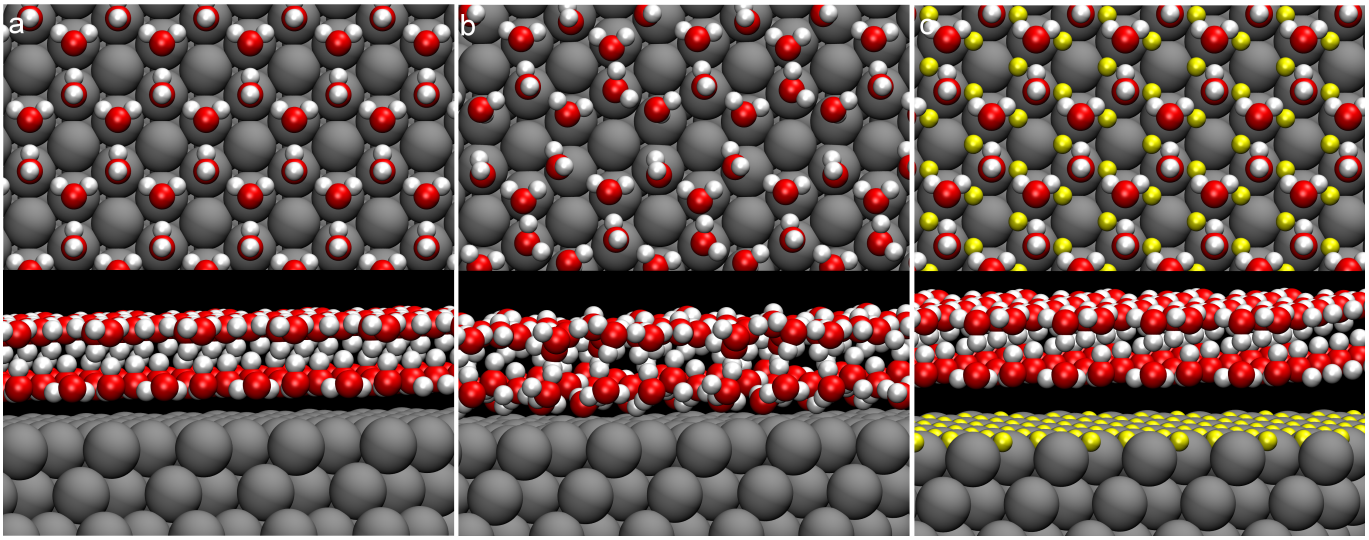

FIG. 1: Snapshots of the initial structure of water on clean platinum (left panels), after 11 ps in the molecular dynamics run (center panels), the initial structure of water on platinum covered with 1 ML of hydrogen (right panels). Only the water bilayer closest to the metal surface, i.e., the first water bilayer, is shown in the top views (upper panels).

ice-like structure has been proposed based on the observation of long-range order of water on metal(111) surfaces and the good match between the lattice constant of metals and the ice-like structure [32] (for reviews, see Refs. [27, 33, 34]).

Furthermore, the experimentally observed work function changes of Au(111), Pt(111) and Ru(0001) upon the adsorption of a water layer can only be theoretically reproduced if this thermal disorder is taken into account [17, 20] which is of crucial importance in electrochemistry since the work function is directly related to the electrode potential [35]. However, for the more strongly interacting substrates Pt(111) and Ru(0001) still a hexagonal arrangement of the water molecules was identified in the AIMD simulations, but the orientation of the water molecules was found to be disordered. This fits nicely to the results of a recent combined low energy electron diffraction (LEED) and He atom scattering study of water on Ru(0001) where the LEED results insensitive to the positions of the hydrogen atoms suggest an ordered structure whereas the He atom scattering results that probe the positions of the hydrogen atoms suggest a disordered structure [36].

Still, in AIMD studies addressing the structure of metal-water interfaces usually no equilibrium coverage of adsorbate layers on the electrode have been considered so far [17, 20, 37–39]. We have therefore extended our previous AIMD study addressing the structure of water at Pt(111) at room temperature by considering different hydrogen coverages in the simulations. Besides considering a fully hydrogen-covered Pt(111) surface with strongly adsorbed hydrogen atom, we have also studied hydrogen-covered Pt(111) with a hydrogen vacancy and with one additional hydrogen atom per surface unit cell.

In this paper, after describing the computational methods, we will present the results of the ab initio molecular dynamics simulations. From the AIMD runs, various distributions have been derived in order to characterize the resulting geometrical structures of the water layers. These will be carefully analyzed and contrasted with existing experimental and theoretical data. Note that this study is part of a long-term project to derive the atomistic structure of the electrochemical double layer at water-metal interfaces by increasing the complexity of the considered interfaces in the calculations in a step-wise fashion [17, 20, 39]. Thus the different factors influencing the structure of the double layer can be disentangled. The dependence of the electrochemical interface on a varying electrode potential will not considered here, however, it is the topic of ongoing research in our lab.

II. COMPUTATIONAL METHODS

All total-energy calculations were carried out using the periodic DFT package VASP [40], employing the generalized gradient approximation (GGA) to describe the exchange-correlation effects by employing the exchange-correlation functional by Perdew, Burke and Ernzerhof (PBE) [41]. It has been shown that this functional gives a reasonable description of the properties of water [42–45]. The ionic cores were represented by projector augmented wave (PAW) potentials [46] as constructed by Kresse and Joubert [47]. The electronic one-particle wave function were expanded in a plane-wave basis set up to an energy cutoff of 400 eV. The Pt(111) substrate was represented by a four-layer slab, of which the outermost two layers were always given full degrees of freedom to move during the geometry optimization and in the molecular dynamics runs as well.

Ab initio molecular dynamics (AIMD) simulations were performed using the Verlet algorithm [48] at a temperature of 300 K within the microcanonical ensemble for at least 11 ps. These simulation times turned out to be long enough to reproduce the main experimental findings of the water-induced work function change on (111) metal surfaces [17, 20]. As a rule of the thumb, the time step in MD simulations should be approximately one-tenth of the shortest period of motion [49]. As far as water is concerned, this corresponds to the O-H stretch vibrational period which is typically about 10 fs. Hence we have chosen a time step of 1 fs. The role of possible quantum effects in the hydrogen dynamics is hard to assess as true quantum dynamical simulations are computationally much too demanding. Tunneling effects are usually negligible due to the large width of barriers, but zero-point effects could become important. Yet, in dissociation and recombination reactions on surfaces involving hydrogen, such as the proton transfer considered in this study, the sum of zero-point energies can stay approximately constant so that the effect of the zero-point energies is rather limited [50].

Note that liquid water described by the PBE functional is overstructured. Therefore, it has been suggested to perform DFT-PBE simulations of liquid water at higher temperatures (see, e.g., [43, 51, 52]). Our goal is not to study liquid bulk water but the structure of water at a platinum electrode, and the water structure at this interface is not only determined by the water-water, but also by the platinum-water interaction. There are indications that the water-metal interaction is slightly underestimated by PBE [45, 53] which would rather suggest to use a lower temperature to appropriately model PBE water-metal interfaces. In the light of these uncertainties we decided not to select some more or less arbitrarily modified temperature, but rather used 300 K. There have been suggestions that the DFT description of water can be improved when dispersion effects are appropriately taken into account [54, 55]. We have also taken steps along this line [45, 56], but this is an issue of ongoing research, in particular as far as the treatment of the screening of the van der Waals interaction inside metal electrodes is concerned [57].

The Pt(111)-water interface was modeled with two water layers within a $2\sqrt{3} \times 2\sqrt{3}R30^\circ$ geometry, leading to 12 metal atoms and 8 water molecules per layer. Energy-minimum structures of the water bilayers were used as the initial configurations of the molecular dynamics runs, and were determined using $4 \times 4 \times 1$ k points until the energies were converged to within 10^{-4} eV. For the molecular dynamics simulations, the energy cutoff was reduced to 350 eV and $2 \times 2 \times 1$ k points were used to obtain a compromise between sufficient accuracy and manageable simulation time. Water layers on Pt(111) in an ultra-high vacuum chamber typically desorb at temperatures below 200 K [58, 59]. Consequently, in order to prohibit the water layers from desorbing in our computational setup, the height of two oxygen atoms per surface unit cell in the second water layer above the surface (but not their lateral position) was fixed. This means that just two out of 144 spatial degrees of freedom of the water layer are not treated dynamically.

III. RESULTS AND DISCUSSION

Before discussing the structure of water layers on hydrogen-covered Pt(111), we first address the structure of water on clean Pt(111) as a reference which was already previously studied by AIMD simulations [17]. The lefthand panels of Fig. 1 show the initial structure of water used in the molecular dynamics run, which we refer to in this paper as the ordered water bilayer structure on Pt(111). It should be noted that for a single water bilayer on Pt(111) it has been shown that the combination of so-called flat-lying and H-down oriented water molecules comprise the stable structure [17] if a $\sqrt{3} \times \sqrt{3}R30^\circ$ periodicity is assumed. He scattering experiments [60] have identified two other water structures on Pt(111) at 130 K, a $\sqrt{37} \times \sqrt{37}R25.3^\circ$ and a $\sqrt{39} \times \sqrt{39}R25.3^\circ$ structure, which have also been addressed in DFT studies [29, 61, 62] and in a recent combined scanning tunneling microscopy (STM) and DFT study [63]. We have not used these larger structures as a basis for our investigation since a second ice-like hexagonal water layer does not fit on top of them [63]. Furthermore, we are mostly interested in general trends in the changes of the water structure on Pt(111) upon introducing a hydrogen adlayer, which we derive from simulations using exactly the same, already rather large unit cell for all considered systems.

The presence of the second bilayer, however, influences the structure of the first water layer. It stabilizes the H-up orientation for the molecules of the first hexagonal bilayer, as the stronger hydrogen bonding between the water molecules in this configuration lowers the total energy. The presence of surrounding water weakens an individual water molecule's bond with the metal surface, of which one consequence is a substantial shift of the position of water from the platinum surface, from 2.4 Å for a single water molecule on platinum to about 3.2 Å for the ordered water bilayers in Fig. 1. In order to maximize the hydrogen bonding in the double-bilayer structure, the two honeycomb lattices of water are stacked directly against each other, but with the water molecules staggered in terms of their relative orientations: H-down-oriented molecules lie right above the flat-lying molecules of the first bilayer, while flat-lying molecules are positioned right above the H-up molecules of the first bilayer.

We are interested in the influence of a hydrogen layer on the water structure at Pt(111) in this study, and a natural choice is the case of a full monolayer of hydrogen on Pt(111) which has been theoretically shown to be stable a room temperature [10, 20]. Hydrogen atoms were placed on fcc threefold-hollow sites since a full monolayer of hydrogen on Pt(111) adsorbs more stably at this po-

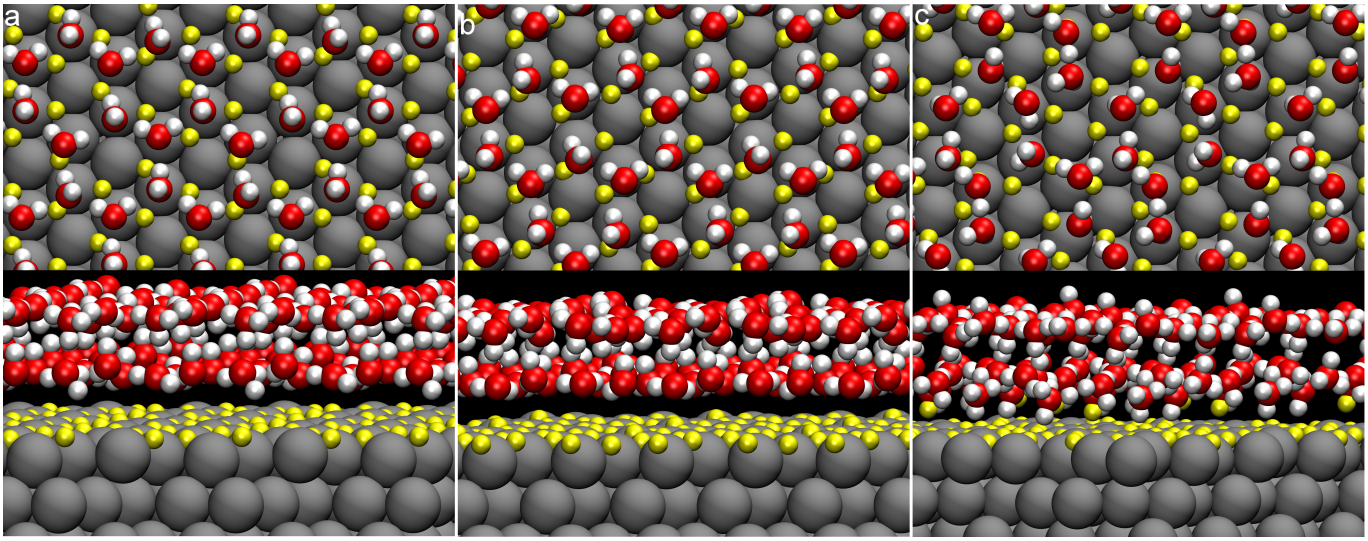

FIG. 2: Snapshots at 11 ps of ab initio molecular dynamics runs of two water layers above a hydrogen-covered Pt(111) electrode. The hydrogen overlayer is drawn using yellow in order to understand the figures better. The simulation for water/H(0.92 ML)/Pt is shown on the left, while the water/H(1 ML)/Pt and water/H(1.08 ML)/Pt systems are shown in the center and righthand panels, respectively. Only the water bilayer closest to the metal surface is shown in the top views (upper panels).

sition [20], compared to analogues for top-site and hcp threefold hollow site adsorption. In addition to the full monolayer of hydrogen, we chose to investigate two others: a slightly lower coverage, $\theta = 11/12$ ML, which was chosen in order to investigate vacancies in a full hydrogen cover, and a higher one, $\theta = 13/12$ ML, which was chosen in order to investigate the behavior of weakly-bound hydrogen atoms, the so-called opd hydrogen.

The initial structures of the water bilayers for the water/hydrogen/Pt systems are shown in Fig. 1(c). The structure of the double bilayer is similar to that shown in Fig. 1(a), except for the fact that the water bilayers are positioned farther away from the metal surface by about 1 Å, which is a substantial shift.

In the presence of the water layers, there are three choices in selecting the position of the hydrogen vacancy in the supercell that was used. The total energies for the three systems were however found to be within 0.005 eV of each other, and so the choice for the location of the hydrogen vacancy is trivial. What is more interesting is the selection of the adsorption position of the weakly-bound opd hydrogen atom for the $\theta = 13/12$ ML hydrogen cover. We likewise have three choices for hcp-site adsorption, and another three choices for top-site adsorption.

Adsorption on the top site located below a flat-lying water molecule was found to be the most energetically favorable for the opd hydrogen atom, and hence this configuration was selected as the initial structure for subsequent molecular dynamics simulations. The two other top-site adsorption configurations, with the hydrogen atom located below an H-up water and on the uncovered Pt atom, are both about 0.02 eV higher in energy. Adsorption energies of the opd hydrogen on an hcp threefold-hollow site were not found to vary greatly on

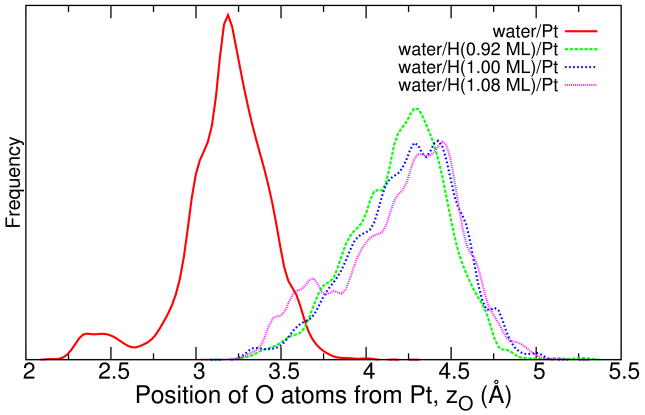

FIG. 3: Distribution function for the distance of the oxygen atoms of the first water bilayer from the platinum surface.

the location choice within the supercell, and are higher in energy by 0.39 eV compared with the most stable top-site adsorption. What makes this interesting is the fact that the trend is reversed in the absence of water above the platinum surface. This suggests that the presence (or absence) of water in the system has a profound effect on the stability of opd hydrogen. On a Pt(111) surface covered with a full monolayer of fcc site-adsorbed hydrogen, we could not obtain stable opd hydrogen adsorption on top sites in the absence of water. Adsorption on the unoccupied hcp sites is on the other hand favorable, but more weakly bound ($E_{ads} = -1.74$ eV) compared with the adsorption of a hydrogen atom on clean platinum (fcc-site, $E_{ads} = -2.60$ eV).

The structures of the water/H/Pt systems at 11 ps are shown in Fig. 2. A quick visual comparison with Fig. 1(c)

shows obvious signs of disorder in the water bilayers. In order to make a more encompassing description of the disorder in these systems, we have plotted distribution functions of some relevant structural parameters of the first water bilayer in order to more clearly see the extent to which the water bilayer is disordered, through the following parameters:

1. Planar deviation. The distances from Pt of oxygen atoms of the ordered water structure shown in Fig. 1 are practically the same all throughout the bilayer. Thermal disorder is measured here as the extent to which oxygen atoms deviate from this planar arrangement.

2. Honeycomb structure deviation. The angle formed by any three oxygen atoms in the top view of Fig. 1 is almost exactly 120°, and so a honeycomb network of perfect hexagons is one of the most obvious characteristics of the ordered bilayer. Disorder is measured here as the extent to which O-O-O angles deviate from 120°.

3. Orientational inhomogeneity. The two criteria mentioned above refer to disorder observable through the relative positions of water molecules in three-dimensional space. Here, disorder is measured by the orientations of water molecules with respect to the surface, and more importantly, with respect to each other.

4. O-H bonding. It is interesting to examine what effect the hydrogen cover has on the OH bonds of the nearest water layer. In particular, proton transfer events at the metal-water interface and within the water molecule network are examined.

The vertical axes of the distribution functions refer to the number of times within the 10 ps timeframe the parameter concerned is found at a given value, omitting the first 1000 fs of the 11 ps run that comprise the thermalization period.

Distributions of oxygen atom positions with respect to the platinum surface are shown in Fig. 3. For comparison, we note that the corresponding distribution function for the ordered water bilayer is a closely-spaced (0.03 Å) double-spike structure at 3.17 Å. There is an observable rightward shift of the peak of the distribution with respect to coverage, the water molecules move farther away from the platinum surface as more hydrogen is added to the water-platinum interface. Furthermore, a decrease in peak height and increase in the distribution spread is found with increasing coverage, indicating that the disorder in the water layer increases as the platinum surface is covered with more hydrogen. For water on clean Pt, the closer proximity of the water layer to the platinum surface as well as the sharper distribution of the oxygen (and hence water molecule) positions are indicative of stronger water-surface interaction compared to the hydrogen-covered counterparts.

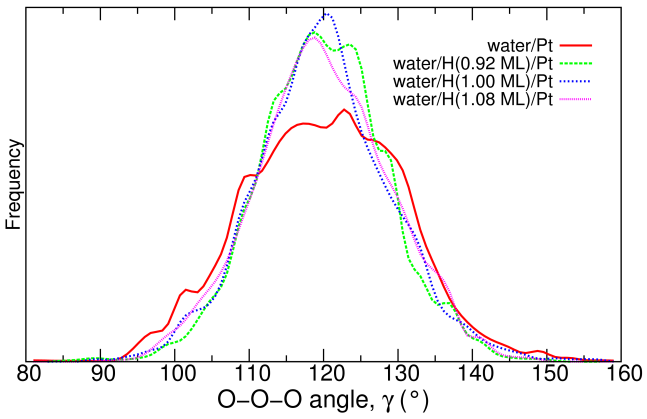

FIG. 4: Distribution function for the angle formed between any given three adjacent oxygen atoms of the first water bilayer.

Aside from the main peak at 3.17 Å for the water/Pt system, we find a minor peak at 2.45 Å. This minor peak is due to single water molecules temporarily breaking out of the bilayer, and has been earlier shown to be correlated with the interaction strength between water and the metal substrate [17]. This minor peak is not observed for the hydrogen-covered platinum surface at the submonolayer and full monolayer coverages investigated here, but is interestingly once again present with the addition of the top site-adsorbed hydrogen atom. As will be discussed later in this paper, this minor peak is relevant in the occurrence of proton transfer in the metal-water interface.

Fig. 4 shows the distribution of angles formed between any given three adjacent oxygen atoms in the first water bilayer. For comparison, we note that the corresponding distribution function for the ordered water bilayer is a sharp spike at 120°, and hence a broader distribution implies greater disorder. More precisely, this angle is obtained from the projected coordinates of the oxygen atoms onto $z = 0$, since the disorder along the surface-normal z direction is already described in Fig. 3. The mean value of all distributions is always 120°, as one can naturally expect from hexagons. We see a clear distinction between the hydrogen-covered and uncovered cases. The important thing to note here is that the presence of the hydrogen layer reduces the disorder in the water bilayer by keeping the honeycomb lattice arrangement of water molecules intact. We surmise that the roughness in what would otherwise be ideal normal distributions is due to the limited molecular dynamics run used.

The orientational distribution of water molecules are expressed in this study through two angles: dipole moment angles α, and HOH plane angles β. The water-surface dipole moment angle α_{w-s} is defined here as the angle that a water molecule's dipole moment vector makes with a surface-parallel plane.

Fig. 5 shows the distribution functions we obtained. The range of angles is from $-90°$ to 90°, with negative

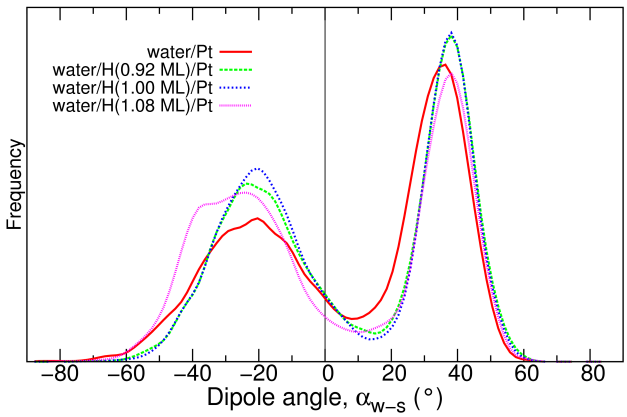

FIG. 5: Distribution function for the dipole angle α_{w-s}, which is the angle formed between the dipole moment vector of a given water molecule and a plane parallel to the platinum surface, e.g. $z = 0$.

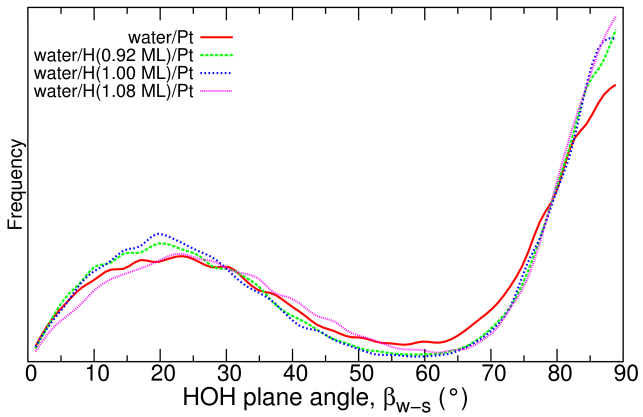

FIG. 6: Distribution function for the water-surface plane angle β_{w-s}, which is the angle formed between the H-O-H plane for any given water molecule and a plane parallel to the platinum surface, e.g. $z = 0$.

angles meaning the z-component of the dipole moment vector of a water molecule is pointing into the surface. The corresponding distribution function for an ordered water bilayer would have sharp spikes at $-20°$ and $38°$, which correspond to the angles made by flat-lying and H-up water molecules, respectively.

The α_{w-s} distribution is especially important because one can estimate the net dipole moment of the water bilayer at room temperature from this. In particular, the mean value we obtained for α_{w-s} for the distribution function of water on the clean platinum surface is $7.6°$, which indicates that the net dipole moment of the bilayer points away from the metal surface. The presence of the hydrogen layer of 1.08 ML lowers this value significantly.

The distributions are far from being flat horizontal lines, meaning the water molecules are far from being randomly oriented. Across all the distributions, we also find that the section centered at $-20°$ is broader than the section with the peak at about $39°$. This means that the initially flat-lying molecules exhibit greater disorder compared to the initially H-up molecules. The role of the hydrogen layers is primarily to make the distributions less broad, hence to decrease the disorder in the water bilayer. Furthermore, the presence of hydrogen leads to a minor shift in the H-up peak toward higher angles.

Water-surface HOH plane angles β_{w-s} on the other hand are the angles created between the plane of the water molecule and a surface-parallel plane such as $z = 0$. We show in Fig. 6 the distributions β_{w-s} for the four systems covered in this study. The corresponding distribution function for the ordered water bilayer would have sharp spikes at -20° and 89°, corresponding to the angles made by flat-lying and H-up water molecules, respectively (simply speaking, while the plane of H-up water is oriented perpendicular to the surface, the flat-lying molecules are not exactly lying parallel to the surface).

Once again, we find that the initially flat-lying molecules exhibit greater disorder compared to the initially H-up molecules, implying that the initially flat-lying molecules have greater freedom to reorient both their dipole vectors and HOH plane. The presence of the hydrogen layer likewise lessens the orientational disorder in the water bilayer as made evident through the higher peaks at $\beta_{w-s} = 20°, 89°$ and narrower distributions.

It is also convenient to look at the α_{w-w} and β_{w-w} distributions shown in Figs. 7 and 8 to complement the previous discussion. These are the intermolecular counterparts of α_{w-s} and β_{w-s}. For example, instead of measuring α with respect to the surface plane, the intermolecule dipole angle α_{w-w} is obtained by comparing a given pair of water molecules, as illustrated in Fig. 9. Here we separate the analysis in terms of the two "layers" that comprise the water bilayer, referring to the initially flat-lying molecules as comprising layer A, and the initially H-up-oriented molecules making up layer B. These are good measures for orientational inhomogeneity as α_{w-s} and β_{w-s} do not distinguish between coordinated and totally independent molecular rotations within each layer.

The corresponding distribution function for an ordered water bilayer would have spikes at $0°$, as the water molecules are perfectly aligned in the ordered bilayer of Fig. 1. The distributions in Fig. 7 and Fig. 8 show that the individual molecules within the water layers are mostly off-aligned in their dipole vectors and HOH planes by 10-20°.

From these distributions we find that layer A (initially flat-lying) exhibits more disorder than layer B (initially H-up), which is consistent with the conclusions we obtained from Fig. 5 and Fig. 6. More importantly, the presence of the hydrogen cover generally lessens the orientational inhomogeneity in the water bilayer. The one exception to this trend is the surprising presence of a peak near $\alpha_{w-w} = 80°$ for the layer B (initially H-up) molecules of the hydrogen (1.08 ML)-covered platinum surface. We attribute the presence of this peak to the disorder in the water bilayer brought about by the pro-

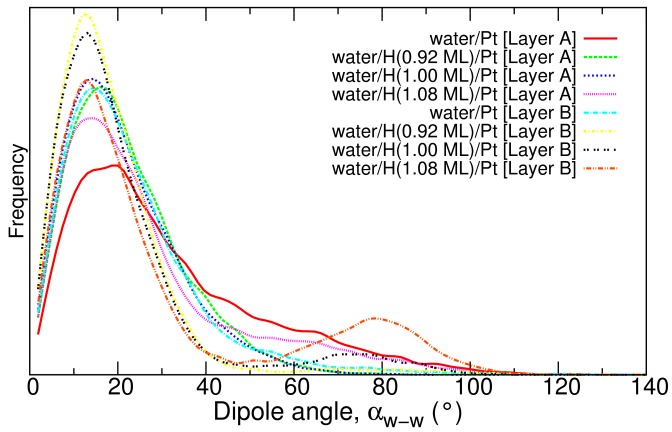

FIG. 7: Distribution function for the intermolecular dipole angle α_{w-w}, which is the angle formed between the dipole moment vectors of any given pair of water molecules (see Fig. 9).

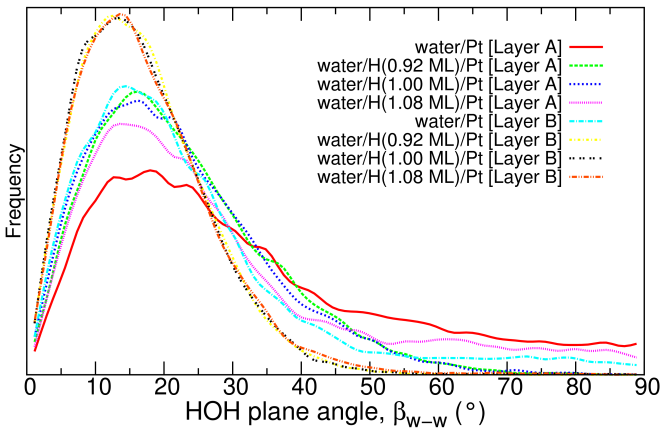

FIG. 8: Distribution function for the intermolecule plane angle β_{w-w}, which is the angle formed between the H-O-H planes of any given water molecule pair.

ton transfer observed in the system, which is discussed in more detail later in this section.

A definite trend for disorder as a function of hydrogen coverage was found with regard to the position of water molecules from the platinum surface. As far as any disorder in the honeycomb structure and the relative orientation is concerned, its dependence on the exact hydrogen coverage is much harder to discern. A larger sampling of data, e.g. through longer molecular dynamics runs may be necessary to make more decisive conclusions on the disorder trend for the three hydrogen coverages near unity.

Typically one would expect that less strongly-bound water layers on the metal surface to be more liquid-like, i.e., to have greater disorder, because of the smaller influence of the surface arrangement on the water structure. It is thus surprising to find more order for the case of water on hydrogen-covered Pt(111). One may argue that the stronger order in the water layer, particularly on the preservation of a honeycomb lattice, is caused by the creation of directed hydrogen bonds between the water molecules and the hydrogen atoms of the adlayer at the fcc sites. This explanation is however unapt given the increase in the water-surface separation upon the formation of the hydrogen adsorbate layer which indicates that no additional hydrogen bonds are formed.

In order to explain these results, it is helpful to look at formation energies for water/Pt and water/H/Pt, which can be obtained using

$$E_{\mathrm{H_2O\text{-}Pt}} = \frac{E(\mathrm{H_2O/Pt}) - [E(\mathrm{Pt}) + NE(\mathrm{H_2O})]}{N} \quad (1)$$

$$E_{\mathrm{H_2O\text{-}H/Pt}} = \frac{E(\mathrm{H_2O/H/Pt}) - [E(\mathrm{H/Pt}) + NE(\mathrm{H_2O})]}{N} \quad (2)$$

where $E_{\mathrm{H_2O\text{-}Pt}}$ is the formation energy of water on a clean platinum surface, $E(\mathrm{H_2O/Pt})$ is the total energy of the system comprised of ordered water bilayers on

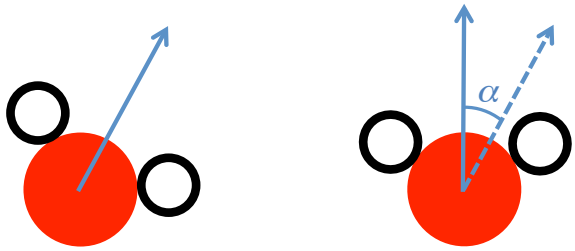

FIG. 9: Defining the intermolecular dipole angle α_{w-w}. The arrow represents the dipole moment vector of a water molecule.

platinum, $E(\mathrm{Pt})$ is the energy of the platinum surface, $E(\mathrm{H_2O})$ is the energy of a water molecule in a vacuum environment, $E_{\mathrm{H_2O\text{-}H/Pt}}$ is the formation energy of water on hydrogen-covered platinum, $E(\mathrm{H_2O/H/Pt})$ is the total energy of the system comprised of ordered water bilayers on hydrogen-covered platinum, $E(\mathrm{H/Pt})$ is the total energy of hydrogen-covered platinum, and N is the number of water molecules in the system.

Formation energies were calculated for the water/Pt and water/H(1 ML)/Pt systems. Surprisingly, very similar numbers were obtained, at -0.58 eV. It is important to note that this energy is based on calculations with two water bilayers. Using just one water bilayer, the formaton energy for the H-down bilayer is only -0.48 eV, very similar to previously reported values [17, 31, 62]. The higher formation energy in the two-layer system is due to the additional hydrogen bonding between the two water bilayers.

It should also be noted that the adsorption energy of a single water molecule on a clean platinum surface is -0.23 eV, and the the larger magnitude of the formation energy is due to the hydrogen bonding. One may interpret the significant increase in the separation between water and hydrogen-covered platinum as evidence for less strongly surface-bound water layers. Given that the two

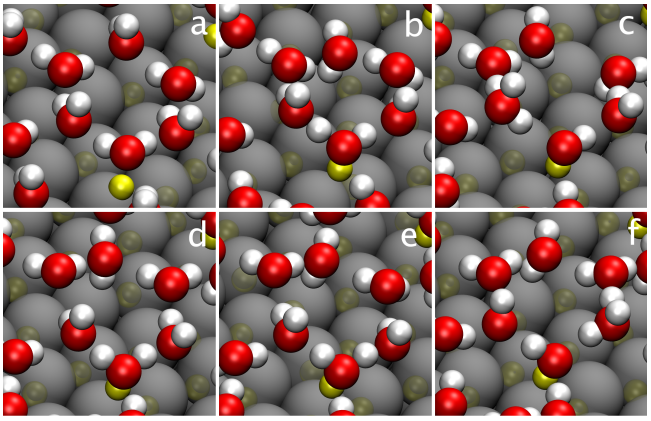

FIG. 10: Snapshots showing proton transfer in the system for water on platinum covered initially by hydrogen at 1.08 ML. The top site-adsorbed hydrogen atom is shown in brilliant yellow in order to distinguish it from the rest of the hydrogen atoms covering the platinum surface. (a)-(b) transfer from the Pt surface to the interface water; (c)-(f) proton transfer within water molecules.

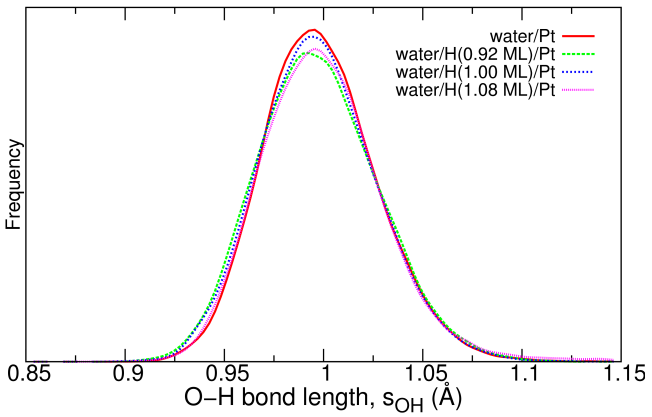

FIG. 11: Distribution function for O-H bond lengths.

calculated formation energies are similar, we can thus say that the unexpected stronger order we find through some of the distribution functions shown for hydrogen-covered platinum arises from the stronger hydrogen bonding between water molecules.

The stronger order in terms of the position of the water bilayer from the metal surface Fig. 3 for water/Pt compared with water/H/Pt is attributed to the stronger interaction with the surface; the stronger order in the water bilayer on the hydrogen-covered platinum in terms of maintaining the honeycomb structure and orientational homogeneity (Figs. 7, 8) is attributed to stronger interaction between water molecules. This is consistent with the fact that hydrogen bonding is highly orientational.

The weak interaction of water with the hydrogen-covered Pt(111) electrode means that for specifically adsorbed atoms and molecules the interaction with water will be even less important than on clean Pt(111) where the influence of the presence of water on chemisorption energies is already minor, as also on other metal surfaces [20]. However, the upd hydrogen layer passivates the Pt(111) electrode, adsorbates have to replace the chemisorbed hydrogen atoms. Furthermore, the electronic properties of Pt(111) will be influenced by the presence of upd hydrogen [64]. The precise influence of the hydrogen upd layer on the electrocatalytic properties of a Pt(111) electrode still need to be studied in detail.

Finally, we would like to comment on proton transfer events that were observed only in the molecular dynamics run with a 1.08 ML hydrogen cover in between platinum and water. Snapshots are shown in Fig. 10. In panel (a) we can see the top-site-adsorbed hydrogen atom still adsorbed on the platinum surface. In panel (b) the top-site adsorbed hydrogen atom moves up to the water layer, as the receiving water molecule prepares to transfer one of its hydrogen atoms to a neighboring water molecule. A series of transfers of hydrogen atoms within the water bilayer is observed, jumpstarted by the initial transfer of hydrogen from the platinum surface.

Aside from the close proximity of the top-site adsorbed opd hydrogen to the water layers, it is also less strongly bound to the platinum surface. Referring to the systems comprised of ordered water bilayers on hydrogen-covered platinum, our calculations show that it needs 2.13 eV to remove the additional weakly bound hydrogen out into the vacuum region (not taking account possible energy barriers), while removing one of the fcc site-bound hydrogen atoms requires 2.59 eV. In contrast to this loosely bound hydrogen, the rest of the hydrogen cover is relatively intact. The presence of water does not shift the hydrogen cover's position from platinum, and the adsorption energy per hydrogen atom for the full monolayer coverage remains at -2.68 eV. Within the limited run time of the molecular dynamics performed, no fcc-bound hydrogen atom was observed to hop out of the fcc threefold-hollow sites. This indicates that the hydrogen upd layer is rather stationary. In contrast, the more weakly bound opd hydrogen seems to be rather mobile. The equilibrium coverage of the opd hydrogen layer obviously consists of hydrogen atoms or protons that dynamically move back and forth between the electrode and the water layers which contributes to their high electrocatalytic activity [22].

Interestingly, the series of proton transfers is not very visible in the OH bond length statistics shown in Fig. 11. This suggests that proton transfer, while shown to occur, is still a relatively rare event if one is to look at all OH bonds in the water layer. Having said that, the hydrogen cover on platinum does not seem to change the OH-bond lengths of water significantly. Proton transfer/exchange in the Pt-water interface is not very likely to occur for hydrogen coverages $\theta \leq 1$ ML.

IV. CONCLUSIONS

In summary, we have performed ab initio molecular dynamics simulations in order to study the structure of water layers on clean and hydrogen-covered Pt(111) electrodes at room temperature. In addition to Pt(111) covered with one monolayer of hydrogen, also hydrogen-covered Pt(111) with a hydrogen vacancy and with one additional hydrogen atom per surface unit cell were considered. In the presence of a hydrogen layer on Pt(111), the distance of the water molecules from the metal atoms is increased by more than 1 Å compared to clean Pt(111) indicative of a weakened water-electrode interaction. Yet, the total formation energy of the water layers is hardly influenced by the presence of the hydrogen layers which suggests that the weakening of the water-electrode interaction is accompanied by a strengthening of the water-water interaction.

All considered water bilayers on clean and hydrogen-covered Pt(111) are more disordered than ice, although far from the liquid state. Surprisingly, a stronger order in the water bilayer on hydrogen-covered Pt(111) in terms of maintaining the honeycomb structure and orientational homogeneity has been found. At room temperature, one would expect less strongly-bound water layers on the metal surface to be more liquid-like, i.e., to have greater disorder, because the water molecules are free to move beyond the periodic constraints of the surface. The opposite result is attributed to the fact that the presence of the hydrogen layer weakens the interaction of the water with the surface, and the resulting stronger water-water interaction promotes the unexpected order in the water bilayer. Thus the presence of the strongly bound upd hydrogen layer passivates the Pt(111) electrode which should also be relevant for its electrocatalytic activity.

The additional weakly bound hydrogen adatom is found to be transferred to the water layer during the 11 ps run time of the AIMD simulations leading to the formation of hydronium complexes. This suggests that the opd hydrogen on Pt(111) is in a dynamical equilibrium with protons in the water contributing to its high electrocatalytic activity.

Acknowledgments

This research has been supported by the German Science Foundation (DFG) through the research unit FOR 1376. Computer time has been provided by the BW-Grid of the federal state of Baden-Württemberg and by a computer cluster financed through the stimulus programme "Electrochemistry for Electromobility" of the German Ministry of Education and Science (BMBF). Useful discussions with Wolfgang Schmickler and Eckhard Spohr are gratefully acknowledged.

[1] D. M. Kolb, Surf. Sci. **500** (2002) 722.
[2] M. Koper, Faraday Discuss. **140** (2008) 11.
[3] A. Groß, Surf. Sci. **500** (2002) 347.
[4] A. Groß, J. Comput. Theor. Nanosci. **5** (2008) 894.
[5] A. Y. Lozovoi, A. Alavi, J. Kohanoff, and R. M. Lynden-Bell, J. Chem. Phys. **115** (2001) 1661.
[6] A. Roudgar and A. Groß, Chem. Phys. Lett. **409** (2005) 157.
[7] J. S. Filhol and M. Neurock, Angew. Chem. Int. Ed. **45** (2006) 402.
[8] C. D. Taylor, S. A. Wasileski, J.-S. Filhol, and M. Neurock, Phys. Rev. B **73** (2006) 165402.
[9] M. Otani and O. Sugino, Phys. Rev. B **73** (2006) 115407.
[10] E. Skúlason, G. S. Karlberg, J. Rossmeisl, T. Bligaard, J. Greeley, H. Jónsson, and J. K. Nørskov, Phys. Chem. Chem. Phys. **9** (2007) 3241.
[11] J. Zhao, C. T. Chan, and J. G. Che, Phys. Rev. B **75** (2007) 085435.
[12] O. Sugino, I. Hamada, M. Otani, Y. Morikawa, T. Ikeshoji, and Y. Okamoto, Surf. Sci. **601** (2007) 5237.
[13] M. Otani, I. Hamada, O. Sugino, Y. Morikawa, Y. Okamoto, and T. Ikeshoji, Phys. Chem. Chem. Phys. **10** (2008) 3609.
[14] J. Rossmeisl, E. Skúlason, M. J. Björketun, V. Tripkovic, and J. K. Nørskov, Chem. Phys. Lett. **466** (2008) 68.
[15] S. A. Wasileski and M. J. Janik, Phys. Chem. Chem. Phys. **10** (2008) 3613.
[16] Y. Gohda, S. Schnur, and A. Groß, Faraday Discuss. **140** (2008) 233.
[17] S. Schnur and A. Groß, New J. Phys. **11** (2009) 125003.
[18] T. Schmidt, P. R. Jr., and N. Markovic, J. Electroanal. Chem. **524** (2002) 252 .
[19] N. M. Marković and P. N. Ross Jr., Surf. Sci. Rep. **45** (2002) 117.
[20] S. Schnur and A. Groß, Catal. Today **165** (2011) 129.
[21] W. Schmickler and E. Santos, *Interfacial Electrochemistry*, Springer, Berlin, 2nd edition, 2010.
[22] E. Santos, P. Hindelang, P. Quaino, E. N. Schulz, G. Soldano, and W. Schmickler, ChemPhysChem **12** (2011) 2274.
[23] R. de Levie, J. Electroanal. Chem. **476** (1999) 92 .
[24] E. Spohr, J. Phys. Chem. **93** (1989) 6171.
[25] K. Raghavan, K. Foster, K. Motakabbir, and M. Berkowitz, J. Chem. Phys. **94** (1991) 2110.
[26] R. Guidelli and W. Schmickler, Electrochimica Acta **45** (2000) 2317.
[27] M. A. Henderson, Surf. Sci. Rep. **46** (2002) 1.
[28] S. Meng, L. F. Xu, E. G. Wang, and S. Gao, Phys. Rev. Lett. **89** (2002) 176104.
[29] S. Meng, E. G. Wang, and S. Gao, Phys. Rev. B **69** (2004) 195404.
[30] G. Materzanini, G. F. Tantardini, P. J. D. Lindan, and P. Saalfrank, Phys. Rev. B **71** (2005) 155414.
[31] A. Michaelides, Appl. Phys. A **85** (2006) 415.
[32] D. L. Doering and T. E. Madey, Surf. Sci. **123** (1982) 305 .
[33] P. A. Thiel and T. E. Madey, Surf. Sci. Rep. **7** (1987) 211.

[34] A. Hodgson and S. Haq, Surf. Sci. Rep. **64** (2009) 381 .
[35] S. Trasatti, Surf. Sci. **335** (1995) 1.
[36] M. Gallagher, A. Omer, G. R. Darling, and A. Hodgson, Faraday Discuss. **141** (2009) 231.
[37] S. Izvekov, A. Mazzolo, K. Van Opdorp, and G. A. Voth, J. Chem. Phys. **114** (2001) 3284.
[38] S. Izvekov and G. A. Voth, J. Chem. Phys. **115** (2001) 7196.
[39] X. Lin and A. Groß, Surf. Sci. **606** (2012) 886.
[40] G. Kresse and J. Furthmüller, Phys. Rev. B **54** (1996) 11169.
[41] J. P. Perdew, K. Burke, and M. Ernzerhof, Phys. Rev. Lett. **77** (1996) 3865.
[42] P. Vassilev, C. Hartnig, M. T. M. Koper, F. Frechard, and R. A. van Santen, J. Chem. Phys. **115** (2001) 9815.
[43] J. VandeVondele, F. Mohamed, M. Krack, J. Hutter, M. Sprik, and M. Parrinello, J. Chem. Phys. **122** (2005) 014515.
[44] B. Santra, A. Michaelides, M. Fuchs, A. Tkatchenko, C. Filippi, and M. Scheffler, J. Chem. Phys. **129** (2008) 194111.
[45] K. Tonigold and A. Groß, J. Comput. Chem. **33** (2012) 695.
[46] P. E. Blöchl, Phys. Rev. B **50** (1994) 17953.
[47] G. Kresse and D. Joubert, Phys. Rev. B **59** (1999) 1758.
[48] L. Verlet, Phys. Rev. **159** (1967) 98.
[49] A. R. Leach, *Molecular Modelling: Principles and Applications*, Pearson, Harlow, 2nd edition, 2001.
[50] A. Groß and M. Scheffler, J. Vac. Sci. Technol. A **15** (1997) 1624.
[51] L.-M. Liu, M. Krack, and A. Michaelides, J. Chem. Phys. **130** (2009) 234702.
[52] M. V. Fernández-Serra and E. Artacho, J. Chem. Phys. **121** (2004) 11136.
[53] P. J. Feibelman, Phys. Rev. B **72** (2005) 113405.
[54] J. Wang, G. Román-Pérez, J. M. Soler, E. Artacho, and M.-V. Fernández-Serra, J. Chem. Phys. **134** (2011) 024516.
[55] A. Poissier, S. Ganeshan, and M. V. Fernandez-Serra, Phys. Chem. Chem. Phys. **13** (2011) 3375.
[56] K. Tonigold and A. Groß, J. Chem. Phys. **132** (2010) 224701.
[57] G. Mercurio, E. R. McNellis, I. Martin, S. Hagen, F. Leyssner, S. Soubatch, J. Meyer, M. Wolf, P. Tegeder, F. S. Tautz, and K. Reuter, Phys. Rev. Lett. **104** (2010) 036102.
[58] E. Langenbach, A. Spitzer, and H. Lüth, Surf. Sci. **147** (1984) 179.
[59] M. Kiskinova, G. Pirug, and H. Bonzel, Surf. Sci. **150** (1985) 319.
[60] A. Glebov, A. P. Graham, A. Menzel, and J. P. Toennies, J. Chem. Phys. **106** (1997) 9382.
[61] P. J. Feibelman, Phys. Rev. Lett. **91** (2003) 059601.
[62] P. J. Feibelman, N. C. Bartelt, S. Nie, and K. Thürmer, J. Chem. Phys. **133** (2010) 154703.
[63] S. Nie, P. J. Feibelman, N. C. Bartelt, and K. Thürmer, Phys. Rev. Lett. **105** (2010) 026102.
[64] B. Hammer, Phys. Rev. B **63** (2001) 205423.